Polymers of Methyl-Substituted *N*-Phenylnorbornene-5,6-dicarboximide: Characterization of Structure and Dynamics

Joel R. Garbow,*,† Jon Goetz,‡ and Jawed Asrar†

Monsanto Company, 800 N. Lindbergh Boulevard, St. Louis, Missouri 63167, and Department of Chemistry, Washington University, St. Louis, Missouri 63130

Received November 10, 1997; Revised Manuscript Received February 25, 1998

ABSTRACT: Synthesis of *N*-phenylnorbornene-5,6-dicarboximide (NDI) with substituents at different positions in the aromatic ring and their polymerization by ring-opening metathesis polymerization (ROMP) leading to high-temperature polymers has been previously described. It was shown that the properties of these polymer are significantly influenced by the size and position of the substituent groups on the ring. This paper describes ROMP of NDI's with methyl substituents at ortho, meta, and para positions. These methyl-substituted polymers show similar trends in mechanical and thermal properties, with ortho substitution raising the temperature of the transition in dynamic modulus and the glass transition temperature, T_g, (stiffening) and meta substitution lowering these transition temperatures (plasticizing effect) relative to unsubstituted PNDI. Solid-state NMR relaxation experiments provide insight into these trends in mechanical and thermal properties. Experiments were performed to measure the carbon laboratory-frame relaxation, T_1(C), and both proton and carbon rotating-frame relaxation, $T_1\rho$(H) and $T_1\rho$(C). The observed trends in these relaxation values are as follows: (a) T_1(C), *o*-CH_3, *m*-CH_3 > PNDI, *p*-CH_3; (b) $T_1\rho$(H), *o*-CH_3 > PNDI, *p*-CH_3, *m*-CH_3; (c) $T_1\rho$(C), *o*-CH_3 > PNDI, *p*-CH_3, *m*-CH_3. We also performed dipolar rotational spin−echo (DRSE) NMR experiments to demonstrate the phenyl rings are flipping in PNDI and *p*-methyl PNDI, but not in either the ortho or the meta isomer. These relaxation results are interpreted in terms of a model which provides a molecular basis for the observed trends in the thermal and mechanical properties of these polymers.

Introduction

Ring-opening metathesis polymerization (ROMP) of *N*-phenylnorbornenedicarboximide has been described in the literature.[1−5] The metal-catalyzed reaction of the *exo* isomer of *N*-phenylnorbornenedicarboximide (NDI) yields a high molecular weight, straight-chain polymer with interesting thermal and thermochemical properties.[1] Melt rheological behavior and the physical and mechanical properties of injection-molded poly(NDI) have been investigated, and a heat distortion temperature in excess of 170 °C has been reported. *In-situ* metathesis polymerization of NDI with unsaturated rubber produces rubber-grafted PNDI, which shows a good balance of high heat and impact properties.[2]

While desirable from a polymer properties point-of-view, polymerization of NDI cannot be easily carried out in the melt, due to the high melt temperature of the monomer. Poor monomer solubility also makes a solution polymerization process using safe solvents relatively difficult. Recently, novel polymers of *N*-phenylnorbornenedicarboximide with fluoro, chloro, and bromo substitution on the phenyl ring have been reported.[6] The properties of the monomers, their polymerization, and the properties of the resulting polymers are all affected by the halogen position (e.g., ortho, meta, para) on the aromatic ring. For example, mixtures of ortho and meta halo-substituted NDI's are found to melt at considerably lower temperatures than either substituted or unsubstituted monomers. Lower melting of the monomer mixture makes it possible to produce copolymers with aromatic substituents by bulk polymerization methods.

In this paper, we describe the preparation and characterization of polymers prepared from NDI monomers having methyl-substituted phenyl rings. As is the case for the halogen-substituted PNDI's, the thermal (e.g, T_g) and thermomechanical (e.g., temperature of tan δ_{max}) properties of polymers prepared from methyl-substituted NDI's are significantly affected by the position of the methyl group on the aromatic ring. To better understand the observed changes in polymer properties which accompany phenyl-ring substitution, a series of methyl-substituted PNDI's was prepared and characterized by solid-state NMR spectroscopy.

Solid-state NMR spectroscopy has been used extensively to study the structure and dynamics of polymers and polymer blends.[7−10] Because solid-state data are sensitive to *intermolecular* as well intramolecular interactions, they can provide important information about chain dynamics and packing in intact polymer systems. Polymer motions in the solid state, which occur over a wide range of frequencies, are important in determining a polymer's bulk mechanical properties. Solid-state NMR relaxation experiments provide a powerful tool for characterizing these motions. In this paper, we describe the results of laboratory-frame (e.g., T_1(C)) and rotating-frame (e.g., $T_1\rho$(H) and $T_1\rho$(C)) NMR relaxation experiments performed on a set of methyl-substituted PNDI's. These experiments probe megahertz-regime and kilohertz-regime motions, respectively, in these polymers. We also discuss the results of dipolar rotational spin−echo NMR experiments which monitor the presence or absence of phenyl-ring flips. The results of these relaxation experiments are integrated into a model for the dynamics of methyl-substituted PNDI's which helps to explain the observed trends in mechanical and thermal properties of these polymers.

Experimental Section

exo-Norbornene-5,6-dicarboxylic anhydride (*exo*-NDA) was prepared by the thermal isomerization of the corresponding

† Monsanto Company.
‡ Washington University.

S0024-9297(97)01656-2 CCC: $15.00
Published on Web 05/27/1998

endo isomer as described by Kastner and Calderon.[11] Aniline, substituted anilines, diethylaluminum chloride, tungsten hexachloride, and acetaldehyde diethyl acetal, which was distilled before use, were purchased from Aldrich Chemical Co.

Catalyst Preparation. In a typical example, 0.563 g of tungsten hexachloride is dissolved in 2.8 mL of toluene. Then 0.4 mL of acetaldehyde diethyl acetal is added to this partly dissolved WCl_6. A reaction takes place between WCl_6 and acetal, releasing HCl and producing a burgundy colored solution. Nitrogen is passed through this solution overnight to remove the HCl.

Synthesis of *N*-(Methylphenyl)norbornenedicarboximides. *N*-(Methylphenyl)norbornenedicarboximides were prepared in a manner very similar to that described previously for the synthesis of *N*-(bromophenyl)norbornenedicarboximides.[6]

Synthesis of PNDI and Methyl-Substituted PNDI Polymers. Ring-opening metathesis polymerization (ROMP) was carried out by dissolving 2.0 g of the desired norbornene-imide in 4 mL of 1,2-dichloroethane. Then 0.1 mL of the catalyst solution (0.5 M tungsten hexachloride in toluene) followed by 0.17 mL of diethyl aluminum chloride (2.05 M solution in heptane) was added to the monomer solution. The polymerization was carried out at 60 °C for 2 h. The polymer was isolated by precipitation of the reaction mixture in methanol. The precipitated polymer was again dissolved in methylene chloride and reprecipitated in methanol, filtered, and dried in a vacuum oven at 60 °C overnight.

Dynamic Mechanical Analysis. Dynamical mechanical analyses (DMA) traces were generated on a Rheometrics II instrument. The temperature was varied at a rate of 3 deg/min. Storage (E') and loss (E'') moduli were measured as a function of temperature from which tan δ (E'/E'') was calculated and plotted.

Differential Scanning Calorimetry. Glass transition temperatures (T_g) were measured on a Perkin-Elmer DSC-2. The temperature was varied from 30 to 300 °C at a rate of 20 deg/min. Samples were encapsulated in standard aluminum DSC pans, and each sample was run twice. Calculations of T_g were performed on an HP1000/LMS system, with T_g defined as the midpoint of the total change in heat capacity. All calculations were performed on the second heat. A pure indium metal standard was used to calculate temperature correction factors.

Solid-State NMR Spectroscopy. Cross-polarization magic-angle spinning (CPMAS) ^{13}C NMR spectra were collected on a Monsanto-built spectrometer operating at a proton resonance frequency of 127.0 MHz. Samples were spun at the magic angle (54.7°) with respect to the static magnetic field in a double-bearing rotor system[12] at a rate of 3 kHz. CPMAS ^{13}C NMR spectra were obtained at 31.9 MHz following 2-ms matched, 50-kHz $^1H-^{13}C$ cross-polarization contacts. High-power proton dipolar decoupling ($H_1(H) = 65$ kHz) was used during data acquisition. Under these conditions, the relative intensities of the peaks observed in each of the spectra accurately reflect the relative amounts of each carbon type present in the samples.[13]

NMR Relaxation Experiments. As described in the Introduction, polymers in the solid state are undergoing motions, over a wide range of frequencies, which are important in determining their mechanical properties. Different frequency regimes can be investigated with different solid-state NMR relaxation experiments. Proton and carbon rotating-frame relaxation, $T_1\rho(H)$ and $T_1\rho(C)$, help to probe low-frequency (kilohertz-regime), cooperative polymer-chain motions while measurements of carbon longitudinal relaxation, $T_1(C)$, are sensitive to higher-frequency (megahertz-regime) motions.

Proton rotating-frame relaxation times, $T_1\rho(H)$, are determined from the decay of carbon signal as a function of $^1H-^{13}C$ contact time, τ, in a CPMAS experiment.[13] $T_1\rho(H)$ is measured in this way to take advantage of the spectral resolution of the ^{13}C NMR experiment. The value $\langle T_1\rho(H)\rangle$ is calculated from a straight-line fit of log(carbon signal intensity) vs τ, where τ varies from 2 to 12 ms. Carbon rotating-frame relaxation times, $T_1\rho(C)$, are determined from the decay of carbon signal as a function of ^{13}C spin-lock time, with the proton rf field turned off, following $^1H-^{13}C$ cross polarization.[14] The value $\langle T_1\rho(C)\rangle$ is calculated from a straight-line fit of log(carbon signal intensity) vs spin-lock time from 0 to 1 ms. $T_1(C)$ experiments were performed according to the method of Torchia.[15] Immediately after cross polarization from protons, the carbon magnetization is restored to the z-axis by a $\pi/2$ pulse. Following a variable waiting period, the remaining magnetization is sampled by a second $\pi/2$ pulse. Phase cycling and data routing are employed to ensure normal inversion−recovery behavior.

Table 1. Substituted PNDI: Molecular Weights, Glass Transitions, Mechanical Loss

sample	M_w (kD)	T_g (°C)	tan δ_{max} (°C)	10× drop in dynamic modulus (°C)
PNDI	100	220	240	232
PNDI, *o*-CH_3	103	248	275	258
PNDI, *m*-CH_3	226	206	222	211
PNDI, *p*-CH_3		222		

Dipolar-Rotational Spin−Echo NMR. Carbon dipolar tensors were characterized by dipolar rotational spin−echo (DRSE)[13,14,16] ^{13}C NMR experiments at 15.1 MHz with magic-angle spinning at 1859 Hz. DRSE is a two-dimensional NMR experiment in which, during the evolution period, carbon magnetization is allowed to evolve under the influence of $^{13}C-^1H$ dipolar coupling while $^1H-^1H$ coupling is suppressed by homonuclear multiple-pulse semiwindowless MREV-8 decoupling. DRSE ^{13}C NMR spectra were obtained following 2-ms matched, 50-kHz $^1H-^{13}C$ contacts with a ^1H decoupling field of 96 kHz. The cycle time for the homonuclear decoupling pulse sequence was 33.6 μs. For singly protonated carbons, a Fourier transform of the intensity at the peak maximum vs evolution time yields a dipolar spectrum consisting of a $^{13}C-^1H$ Pake doublet, scaled by the MREV-8 decoupling, and broken into sidebands by the magic-angle spinning. Molecular motion modifies DRSE sideband patterns[10] just as it does quadrupolar line shapes.[17]

Results

Figure 1 (bottom) shows dynamic mechanical loss curves for PNDI, *o*-CH_3−PNDI, and *m*-CH_3−PNDI measured using a Rheovibron at a frequency of 11 Hz. In measuring these curves, the temperature was varied at a rate of 3 deg/min. As can be clearly seen in these data, the drop in the dynamic modulus for PNDI takes place at a temperature intermediate between that for the *o*-CH_3 and *m*-CH_3 substituted polymers. Corresponding tan δ curves for these three polymers are shown in Figure 1 (top). As with Figure 1 (bottom), the curve for unsubstituted PNDI falls between that of the *o*-CH_3 and *m*-CH_3 PNDI's, with the temperature of tan δ_{max} for PNDI being intermediate to that in the *o*-methyl and *m*-methyl polymers. These mechanical data, together with molecular weights (M_w) and values of T_g for each of the PNDI polymers, are shown in Table 1. The trends observed for the methyl-substituted PNDI's are consistent with those previously reported for halogen-substituted PNDI's.[6] The measured T_g and tan δ values for the *p*-CH_3 material are nearly indistinguishable from that of the unsubstituted PNDI, and values for the *m*-CH_3 polymer are shifted to lower temperature, while those for *o*-CH_3−PNDI are shifted to higher temperature relative to the parent PNDI polymer. In all four of these PNDI polymers, the cis/trans ratios, as measured by high-resolution, solution-state NMR, are approximately 2:3.

Figure 2 shows the cross-polarization magic-angle spinning (CPMAS) ^{13}C NMR spectrum of PNDI. Three

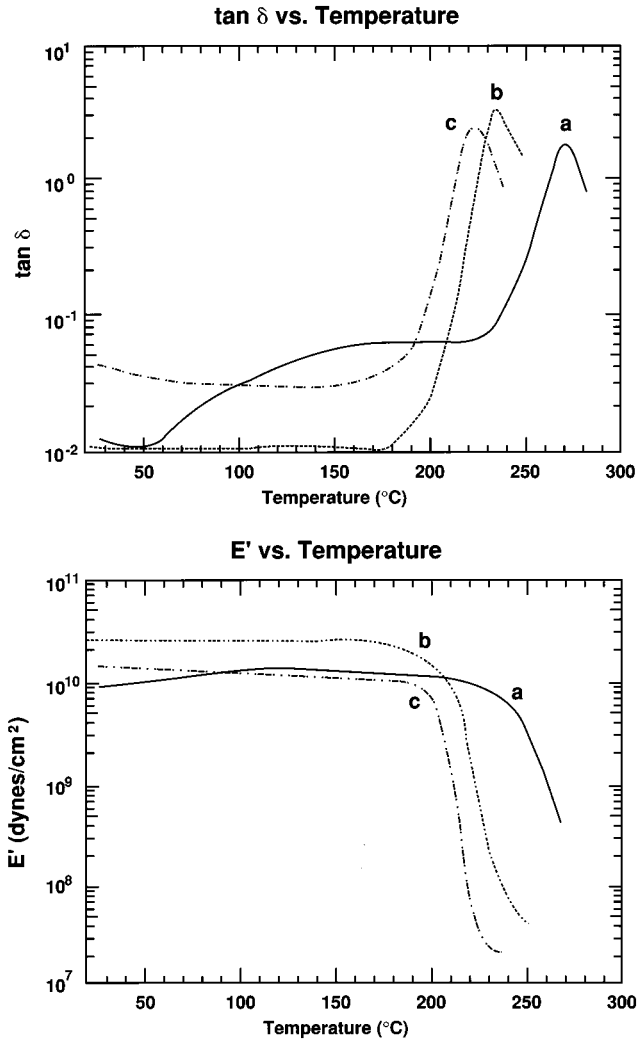

Figure 1. Bottom: Dynamic modulus vs temperature for PNDI (**b**), *o*-CH_3−PNDI (**a**), and *m*-CH_3−PNDI (**c**) measured using a rheovibron at 11 Hz. The temperature was varied at a rate of 3 deg/min. Top: tan δ vs temperature for PNDI (**b**), *o*-CH_3−PNDI (**a**), and *m*-CH_3−PNDI (**c**), measured as described above.

major resonances, arising from carbonyl ($\delta_c = 177$ ppm), aromatic/olefinic ($\delta_c = 128$ ppm), and aliphatic ($\delta_c = 51$, 44 ppm) carbons are seen in this spectrum. Smaller resonances labeled with asterisks (*) are spinning sidebands arising from the mechanical sample rotation.

The CPMAS ^{13}C NMR spectrum of *m*-CH_3−PNDI is shown in Figure 3 (bottom). This spectrum is similar to that of Figure 2 with the addition of a resolved signal due to the methyl group ($\delta_c = 21$ ppm). In addition, there are minor differences in the line shape of the aromatic/olefinic region, reflecting both the covalent attachment of the methyl group and changes in the packing of the PNDI polymer chains caused by the presence of the methyl groups. The CPMAS ^{13}C NMR spectra of *o*-CH_3 and *p*-CH_3−PNDI (data not shown) are very similar to that of Figure 3 (bottom). Figure 3 (top) shows the delayed-decoupling ^{13}C NMR spectrum of *m*-CH_3−PNDI. In collecting these data, a 50-μsec delay was inserted after the cross polarization period before applying the high-power dipolar decoupling field. Only signals from nonprotonated carbons survive this 50-μsec delay. Signals due to carbonyl carbons and two nonprotonated aromatics, the point of attachment of the aromatic ring to the polymer chain and the site at which

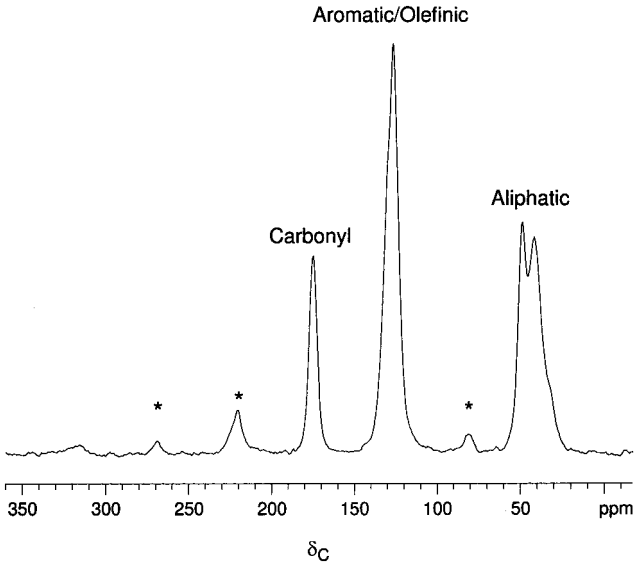

Figure 2. Cross-polarization magic-angle spinning (CPMAS) ^{13}C NMR spectrum of PNDI. The sample was spun at the magic-angle (54.7°) with respect to the static magnetic field in a double-bearing rotor system at a rate of 3 kHz. This CPMAS ^{13}C NMR spectrum was obtained at 31.9 MHz following a 2-ms matched, 50-kHz ^1H-^{13}C cross-polarization contact. High-power proton dipolar decoupling (H_1(H) = 65 kHz) was used during data acquisition.

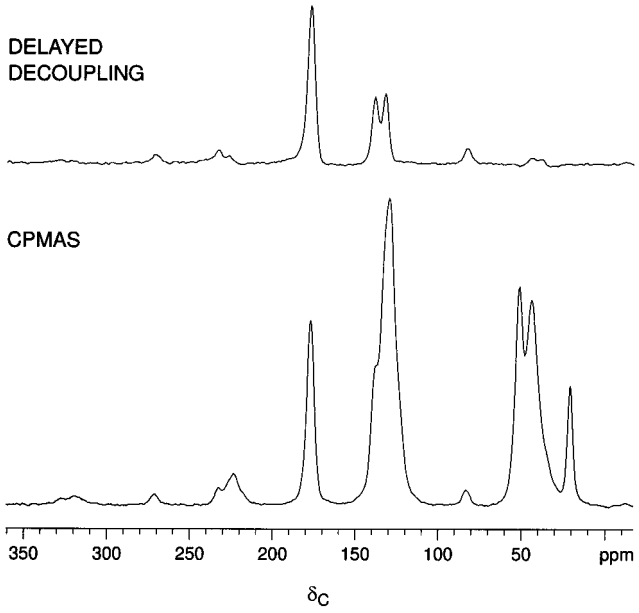

Figure 3. CPMAS ^{13}C NMR spectra of *m*-CH_3−PNDI: (bottom) conventional, as described in Figure 2; (top) delayed decoupling, collected by inserting a 50-μs delay after the cross-polarization period before applying the high-power dipolar decoupling field. Only signals from nonprotonated carbons survive this 50-μs delay.

the methyl groups are attached, are clearly visible in this spectrum.

To characterize the dynamics of these PNDI polymers, we performed a wide variety of solid-state NMR experiments. Table 2 summarizes $\langle T_1\rho(H)\rangle$ and $\langle T_1\rho(C)\rangle$ values for these polymers. These experiments were all performed at an rf-field strength (H_1) of 50 kHz. The $T_1\rho$(C) results reported in this table were measured on the 128-ppm aromatic-carbon line. From these data, we can clearly distinguish between *o*-CH_3−PNDI and the other three PNDI's, whose relaxation behavior is quite

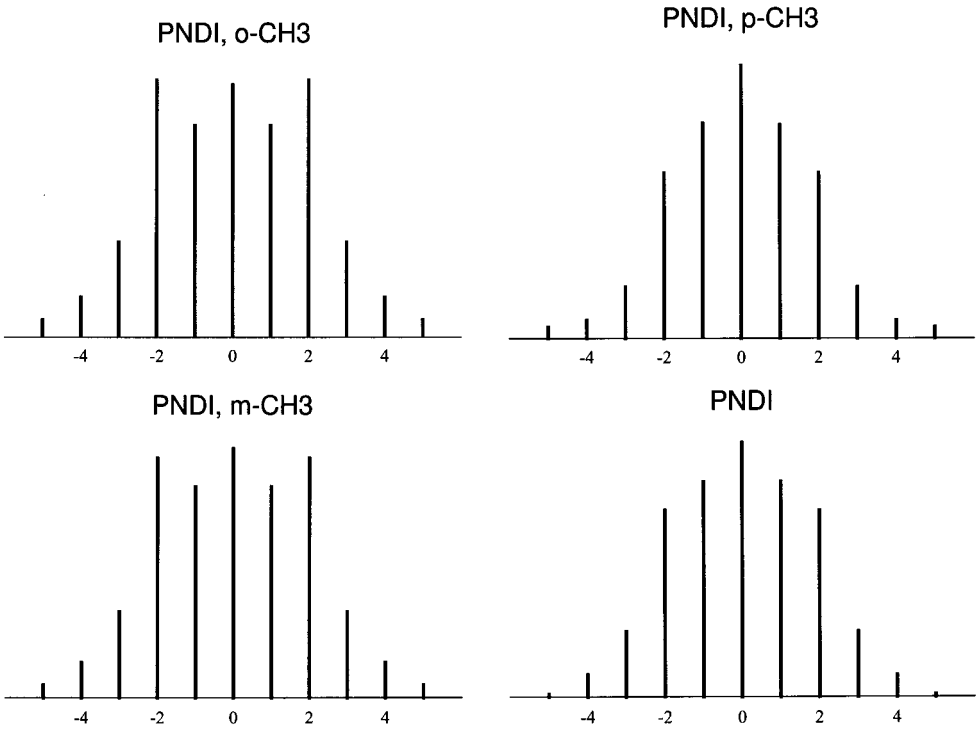

Figure 4. Dipolar rotational spin−echo (DRSE) patterns: (bottom, right) PNDI; (top, right) *p*-CH_3−PNDI; (bottom, left) *m*-CH_3−PNDI; (top, left) *o*-CH_3−PNDI.

Table 2. PNDI: Rotating-Frame Relaxation

sample	$\langle T_1\rho(H)\rangle$ (ms)	$\langle T_1\rho(C)\rangle$ (ms)[a]
PNDI	9	12
PNDI, *o*-CH_3	60−65	>100
PNDI, *m*-CH_3	11	13
PNDI, *p*-CH_3	12	14

[a] 128 ppm, aromatic carbon resonance; $H_1(C) = 50$ kHz.

Table 3. PNDI: Carbon Rotating-Frame Relaxation

	$\langle T_1\rho(C)\rangle$ (ms)[a]			
sample/$H_1(C)$	37 kHz	44 kHz	50 kHz	58 kHz
PNDI	10	11	12	13
PNDI, *o*-CH_3	45	>75	>100	>100
PNDI, *m*-CH_3	9	11	13	16
PNDI, *p*-CH_3	14	13	14	15

[a] 128 ppm, aromatic carbon resonance.

similar. To further probe the dynamics of these PNDI's, we measured $\langle T_1\rho(C)\rangle$ as a function of rf field strength, H_1, ranging from 37 to 58 kHz. These data are reported in Table 3. Here it can be seen that the H_1-dependence of $T_1\rho(C)$ is weak for PNDI and *p*-CH_3−PNDI, while the H_1-dependence for the *m*-CH_3 polymer is strong, with $\langle T_1\rho(C)\rangle$ variations as a function of carbon rf field strength falling between linear ($\propto H_1(C)$) and squared ($\propto H_1^2(C)$) dependence.

As described in the Experimental Section, rotating-frame experiments measuring $T_1\rho(H)$ and $T_1\rho(C)$ are sensitive to motions at midkilohertz frequencies. By contrast, laboratory frame relaxation experiments probe motions in the megahertz regime. Laboratory-frame carbon relaxation, $T_1(C)$, results are reported in Table 4 for the aromatic/olefinic carbon resonance at 128 ppm. Rather than reporting an average relaxation time, $\langle T_1(C)\rangle$, this table reports the fraction of signal which has *decayed* after 1 s. Thus the PNDI and *p*-CH_3−PNDI polymers, for which approximately one-third of the initial signal has decayed after 1 s, show considerably more efficient relaxation than the *o*- and *p*-methyl PNDI's, for which only 10−15% of the signal has decayed.

Table 4. PNDI: Laboratory-Frame Carbon Relaxation

sample	% signal decay after 1 s[a]
PNDI	37
PNDI, *o*-CH_3	11
PNDI, *m*-CH_3	14
PNDI, *p*-CH_3	33

[a] 128 ppm, aromatic carbon resonance.

It has been previously suggested that differences in the mechanical and thermal properties of substituted PNDI polymers were due, in part, to whether their phenyl rings were undergoing ring flips.[6] Dipolar-rotation spin−echo (DRSE) NMR[14,16] is an experiment ideally suited to probe the question of phenyl-ring motion in these polymers. DRSE ^{13}C NMR allows the dipolar coupling between a carbon nucleus and its attached proton to be measured under magic-angle spinning conditions. Resulting dipolar sideband patterns for PNDI and its three methyl-substituted isomers are shown in Figure 4. In the absence of molecular motion, the expected DRSE pattern is a standard Pake doublet, broken up into a series of spinning sidebands. This is exactly the pattern observed in Figure 4 for *m*-CH_3− (left, bottom) and *o*-CH_3−PNDI (left, top). From these patterns, we conclude the phenyl rings in these two polymers are static. By contrast, the DRSE patterns for PNDI (right, bottom) and its *p*-methyl isomer (right, top) are narrowed considerably and are consistent with those expected for phenyl rings undergoing 180 flips, as has been seen previously in Bisphenol A−polycarbonate.[16] These DRSE patterns actually show somewhat more centerband intensity than would be expected for a carbon undergoing π-flips, owing to the contribution from nonprotonated carbons (having no dipolar coupling to a nearby proton) which overlap with

the protonated aromatics in the ^{13}C NMR spectra. Not surprisingly, the observed T_1(C) data (Table 4) correlate with the DRSE patterns of Figure 4, with more efficient T_1 relaxation observed in those PNDI's in which the phenyl rings flip.[18]

Discussion

As summarized in Table 1, the mechanical and thermal properties of *o*-CH_3− and *m*-CH_3−PNDI move in opposite directions relative to PNDI itself, while those of *p*-CH_3−PNDI are indistinguishable from the parent polymer. The observed differences in mechanical and thermal properties in these PNDI polymers cannot be attributed to differences in their molecular weights (Table 1), since above M_w of ∼35K, these bulk properties are molecular-weight independent.[19] Nor can the bulk properties differences be due to differences in polymer cis/trans ratio, since this ratio is the same (2:3) in all PNDI's. Rather, the differences in their bulk properties can be attributed to differences in the position of the methyl substitution on the phenyl ring.

The shift upward in T_g and the temperature of the mechanical loss peak for *o*-CH_3−PNDI is not surprising and can be explained on the basis of steric effects. Calculations show significant steric interaction between the attached methyl group on the phenyl ring of this polymer and the dicarboximide ring.[20] This interaction can easily lead to an overall stiffening of the polymer, which in turns shifts T_g and mechanical loss to higher temperatures. NMR relaxation data presented in Tables 2-4 and Figure 4 provide strong support for this model. The long relaxation times at both kilohertz- and megahertz-frequency regimes and the absence of any significant phenyl-ring motion are consistent with a stiff, sterically hindered polymer.

The presence of a methyl group in the para position on the phenyl rings has no observable effect on either the thermal or mechanical properties of the PNDI polymer. This is mirrored in the NMR results, where we see laboratory-frame and rotating-frame relaxation for *p*-CH_3−PNDI which is indistinguishable from that for the parent polymer. Phenyl rings in both PNDI and its *p*-CH_3 isomer are undergoing π flips. The polymer whose observed properties and NMR relaxation behavior need still be explained is *m*-CH_3−PNDI.

As noted in Figure 1 and Table 1, methyl substitution on the phenyl ring lowers both T_g and the temperature of the mechanical loss peak. These results are consistent with those reported previously for PNDI polymers with halogen-substituted rings.[6] For these chloro, fluoro, and bromo polymers, the drop in the temperature of tan δ_{max} and glass transition temperatures was attributed to increased free-volume created by the bulky halogen groups. A similar explanation can be put forth for the behavior of *m*-CH_3−PNDI. Support for this idea is also found from rotating-frame ^{13}C NMR relaxation data reported in Table 3. Here, the strong H_1-dependence of $\langle T_1\rho(C)\rangle$ indicates the presence of considerable low-frequency motions in this polymer, an observation consistent with the free-volume explanation. However, if placing a CH_3−group in the meta position on the phenyl ring produces a polymer with increased free volume, how do we understand the T_1(C) results and DRSE pattern for this polymer?

As noted previously, the phenyl rings in *m*-CH_3−PNDI are not undergoing π flips, an observation consistent with the long T_1 of its phenyl carbons. Yet we might expect the increase in free volume which is responsible for the decreased temperatures for T_g and tan δ in this polymer might actually make it *more likely* the ring would flip. The molecular models shown in Figure 5 explain the absence of ring flips in this polymer. Figure 5 (bottom) shows a model of the ring-flip process in *p*-CH_3−PNDI. As this figure illustrates, π flips of the phenyl rings is a process which conserves energy. By contrast, π flips of the aromatic rings in *m*-CH_3, while energy-conserving for an isolated chain, are nonenergy-conserving in the bulk polymer. Packing effects from neighboring chains in *m*-CH_3−PNDI inhibit the flipping of the polymer's aromatic rings. A similar effect has been seen in polycarbonate having fluoro-substituted phenyl rings, where again the rings are static because the ring-flip process does not conserve energy.[21] The thermal, mechanical, and NMR data are thus all consistent with a model in which CH_3 groups in the meta position on the phenyl rings help to carve out extra space (i.e., increased free volume), but render the basic π-flip process non-energy-conserving.

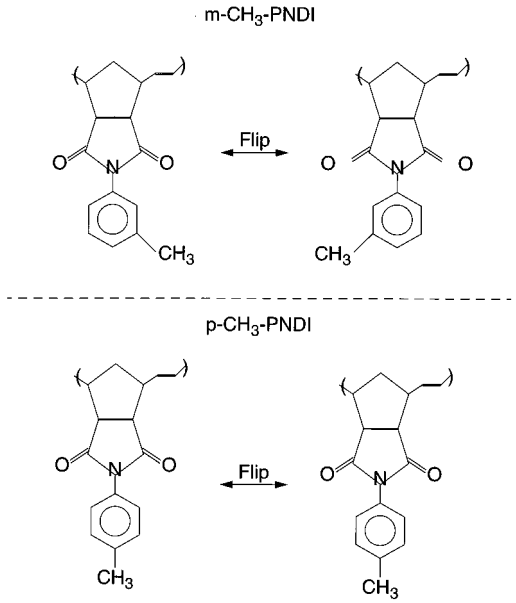

Figure 5. Model of ring-flip process in *p*-CH_3−PNDI (bottom) and *m*-CH_3-PNDI (top).

Acknowledgment. We thank Jeff Hurlbut (Solutia, Inc.) for performing the mechanical and thermal analyses and Professor Jacob Schaefer (Washington University) and Dr. David Snyderman (Monsanto) for many helpful discussions. Work performed at Washington University was supported, in part, by the National Science Foundation, Grant DMR-9015864.

References and Notes

(1) Asrar, J. *Macromolecules* **1992**, *25*, 5150.
(2) Asrar, J.; Hurlbut, J. B. *J. Appl. Polym. Sci.* **1993**, *50*, 1727.
(3) Bazan, G. C.; Schrock, R. R.; Cho, H. N.; Gibson, V. C. *Macromolecules* **1991**, *24*, 4495.
(4) Asrar, J. (Monsanto Company), U.S. Patents 4,965,330, 1990, and 5,049,632, 1991.
(5) Asrar, J.; Hardiman, C. J. (Monsanto Company), U.S. Patent 5,117,327, 1992.
(6) Asrar, J. *Macromolecules* **1994**, *27*, 4036.
(7) Komoroski, R., Ed.; *High-Resolution NMR Spectroscopy of Synthetic Polymers*; VCH: Deerfield Beach, FL, 1986.
(8) Fedotov, V. D.; Schneider, H. *Structure and Dynamics of Bulk Polymers by NMR-Methods*; Springer-Verlag: Heidelberg, Germany, 1989.

(9) Schmidt-Rohr, K.; Spiess, H. W. *Multidimensional Solid-State NMR and Polymers*; Academic Press: San Diego, CA, 1994.
(10) Stejskal, E. O.; Memory, J. D. *High-Resolution NMR in the Solid State*; Oxford Press: Oxford, England, 1994.
(11) Kastner, K. F.; Calderon, N. *J. Mol. Catal.* **1982**, *15*, 47.
(12) Schaefer, J.; Garbow, J. R.; Stejskal, E. O.; Lefelar, J. A. *Macromolecules* **1987**, *20*, 1271.
(13) Stejskal, E. O.; Schaefer, J.; Steger, T. R. *Faraday Symp. Chem. Soc.* **1979**, *13*, 56.
(14) Schaefer, J.; McKay, R. A.; Stejskal, E. O.; Dixon, W. T. *J. Magn. Reson.* **1983**, *52*, 123.
(15) Torchia, D. A. *J. Magn. Reson.* **1978**, *30*, 613.
(16) Schaefer, J.; Stejskal, E. O.; McKay, R. A.; Dixon, W. T. *Macromolecules* **1984**, *17*, 1479.
(17) Spiess, H. W. *Colloid Polymer Sci.* **1983**, *261*, 193.
(18) Klug, C. A.; Zhu, W.; Tasaki, K.; Schaefer, J. *Macromolecules* **1997**, *30*, 1734.
(19) Asrar, J. Unpublished results.
(20) The calculated barrier to phenyl-ring rotation in *o*-CH_3−PNDI is similar to those previously reported in ref 6 for halogen-substituted PNDI polymers.
(21) Schaefer, J. Personal communication.

MA971656O